CMIP6 wave climate simulation in the European North East Atlantic Basin using WaveWatch III

Ponni Maya and Matias Alday Gonzalez and Andrei Metrikine and George Lavidas

Abstract— **Climate change is expected to have an impact on wind patterns, and therefore the generation of waves. Phase 6 of the Coupled Model Intercomparison Project (CMIP6), provides various realization of outputs integrated global coupled models for different centuries. Wind quality is a cornerstone for wave energy as it is the primary generation driver in any wave model. Therefore, proper quantification of wind wave interactions are key in the evaluation of future wave energy potential. In this study, a wave hindcast for the North-East Atlantic, using the WaveWatchIII model forced by CMIP6 winds is presented. The model uses a grid of 0.25° of spatial resolution, covering a longitude range of -21.0° to 10° (west to east) and a latitude range of 18° to 80° (south to north).**

The main objective of this work is to assess the quality of historical winds from all the CMIP6 wind data that are available under the first realization criteria (r1i1p1f1) at the time of this study. This leads to understanding limitations and proposing a selection method to choose the optimal wind dataset to force the wave model within the analyzed area.

Thus, the optimal CMIP6 historical winds for the North-East Atlantic are used to create a 10 years hindcast(from 2003 to 2012). To further assess the suitability of the selected winds dataset for wave generation, results are compared with the ERA5 wave product. The available CMIP6 models show region-specific variations depending on the Regional Climate models used for their developments. The results show the impact of zonal and, meridional wind intensities, on wave characteristics in different regions over the domain.

Keywords— **Climate, CMIP6, WaveWatchIII, Wind.**

I. Introduction

Amidst the backdrop of our changing climate, there is an increasing interest in renewable energy resources that have the capacity to ignite the future with reduced carbon emissions [1]. In this regard, recent studies have suggested that the future of our resources lies in the wind and waves above the subtropical regions [2]. As the impacts of climate change continue to be felt across the globe, it is becoming increasingly clear that these subtropical regions are particularly susceptible to the effects of oceanic and atmospheric interactions, and environmental factors, which can have profound impacts on weather and climate patterns [3][4][5][6][7][8].

Ocean surface waves are linked to the interaction between the atmosphere and the sea surface. In particular, the winds that have been affected by the changing climate, play a vital role in shaping the patterns of waves that propagate across the globe. In the collaborative endeavor to access and enhance comprehension of climate change across temporal planes, known as the Coupled Model Intercomparison Project (CMIP) stands as a pivotal framework.

A recent study by [9] found that sea surface height and zonal wind stress in the equatorial Indo-Pacific are consistent across different spatio-temporal scales in CMIP models. Zelinka et al [10] conducted climate sensitivity research and reported that the multi-model mean and inter-model variance of cloud feedback in CMIP6 are statistically significant with 95% confidence, which explains the results obtained in CMIP5. Tokarska et al [11] examined the warming trends in recent decades in both CMIP5 and CMIP6 models and found that the latter exhibit notably higher climate sensitivity and project greater warming scenarios. Therefore, the accurate quantification of the intricate interplay between wind and waves is imperative in the assessment of the future potential for wave energy.

Several studies, such as those by [12][13][14], have used common statistical methods like bias, standard deviation, and NRMSE to classify the CMIP6 models. However, these methods have been found to be time-consuming and are influenced by the spatial and temporal scales under consideration. In this study, we aim to overcome these

©2023 European Wave and Tidal Energy Conference. This paper has been subjected to single-blind peer review.

The work has been conducted as part of the EU-SCORES project has received funding from the European Union's Horizon 2020 research and innovation programme under grant agreement No 101036457

Ponni Maya (email: p.maya@tudelft.nl) is a Ph.D. candidate at the Marine Renewable Energies Lab (www.tudelft.nl/ceg/mrel), Matias Alday Gonzales is a Post Doctoral Researcher, George Lavidas (email: g.lavidas@tudelft.nl) is an Assistant Professor and Prof. Andrei Metrikine (email: a.metrikine@tudelft.nl), they are part of at the Department of Hydraulic Engineering, Faculty of Civil Engineering and Geosciences, Delft University of Technology

Digital Object Identifier: https://doi.org/10.36688/ewtec-2023-153

limitations by adopting a K-Dimensional Tree approach for classification.

As climate change continues to cause shifts and intensification in wind patterns, the corresponding changes in wave characteristics could significantly impact the potential for wave energy generation [15][16][17][18][19]. This impact could be either positive or negative and is largely dependent on the prevailing conditions and unique location [20] .

In the present study, the WWIII model was utilized to undertake an assessment of the wind data obtained from CMIP6 models, and the preliminary hindcast results are assessed with the cross-model comparison with ERA5.

II. MODEL AND METHODOLOGY

A. Selection of the optimal CMIP6

All models under the first realization (r1i1p1f1) with 3hourly temporal resolution were considered for the study and presented in Table 1. Historical data from the first realization of 11 available model datasets have been analyzed, with a focus on zonal and meridional wind components. Leap days were removed from the 11 CMIP6 model datasets, and the data were resampled to a 6-hourly temporal resolution for comparison with satellite data. We utilized decision tree algorithms, consisting of specifically K-nearest neighbors (KNN) and decision tree [21], with the goal of identifying the most suitable climate model CMIP6 wind datasets that closely resemble the Copernicus Marine Environment Monitoring Service satellite data in the North Atlantic and European regions. Previous studies employed various statistical techniques to arrive at a conclusion. In contrast, the decision tree algorithm is a data structure that partitions space in multidimensional settings, enabling a more efficient and quantitative approach to draw conclusions.

B. K Dimensional Tree (KD Tree)

KD Tree is a technique that integrates the strengths of KNN and decision tree algorithms to structure multi-dimensional data. The decision tree-like structure and fast search capabilities make it an adequate choice for data classification and grouping [22].

The algorithm begins at the root node and descends the tree, evaluating only the relevant branches that contain potential neighbors. This approach results in a significant reduction in search space, especially for high-dimensional data sets. In this case, we employed the Euclidean distance technique (1) to identify the nearest neighbor that is in closer proximity to the satellite measurements, when compared to all the available CMIP6 winds. This approach is described by the equation (1).

$$d(x,y) = \sqrt{\sum_{i=1}^{n}(y_i - x_i)^2} \quad (1)$$

For the analyzed, the optimal dataset is MIROC6, the Model for Interdisciplinary Research on Climate version 6, which is a collaborative climate model developed by multiple institutions in Japan [23]. It is a prominent participant in the Coupled Model Intercomparison Project Phase 6 (CMIP6), which aims to enhance our understanding of climate dynamics and refine projections of future climate change [24].

TABLE I
CMIP6 MODELS AND INSTITUTION

MODEL	INSTITUTION
IPSL-CM6A-LR	Institut Pierre-Simon Laplace, Paris, France
GFDL-ESM4	NOAA, Geophysical Fluid Dynamics Laboratory, Princeton, USA
MPI-ESM1-2-LR	Max Planck Institute for Meteorology, Hamburg, Germany
AWI-ESM-1-1-L R	Alfred Wegener Institute, Helmholtz Centre for Polar and Marine Research, Germany
MIROC6	Japan Agency for Marine-Earth Science and Technology
IPSL-CM5A2-IN CA	Institut Pierre Simon Laplace, Paris, France
MPI-ESM-1-2-H AM	ETH Zurich, Switzerland
GFDL-CM4.gn	NOAA, Geophysical Fluid Dynamics Laboratory, Princeton, USA
GFDL-CM4.gr	NOAA, Geophysical Fluid Dynamics Laboratory, Princeton, USA
CMCC-CM2-SR5	Fondazione Centro Euro-Mediterraneo sui Cambiamenti Climatici, Lecce, Italy
CMCC-ESM2	Fondazione Centro Euro-Mediterraneo sui Cambiamenti Climatici, Lecce, Italy

MIROC6 has a spatial resolution of 2° × 2° and a temporal resolution of 3-hour intervals. For this particular study, the region of interest is defined by a longitude range of -21.0° to 10° (west to east) and a latitude range of 18° to 80° (south to north). By incorporating MIROC6 data into WWIII, the study aims to gain insights into the observed variations in wave climate within this specified geographic area for a period of 10 years.

C. WAVEWATCHIII Model (WWIII)

This study employs WWIII v6.04, a third-generation spectral wind wave model developed by the National Oceanic and Atmospheric Administration's National Centers for Environmental Prediction (NOAA/NCEP). The model is phased averaged and solves the action density balance equation (2).

The equation presented as Equation 2 represents the conservation of wave action in the WWIII model, which is a fundamental aspect of wave energy analysis. In this

equation, the left-hand side consists of several terms that contribute to the overall energy associated with the waves. The second and third terms on the left-hand side correspond to the divergence of wave action flux. These terms indicate how the wave action density is distributed across space, capturing the spatial variations in wave energy propagation and dissipation.

The fourth and fifth terms on the left-hand side represent the partial derivatives of the wave action density N with respect to the spectral width σ and the spectral peak direction θ, respectively. These terms account for how changes in the spectral characteristics of the waves impact the wave action density.

The first term on the left-hand side represents the time derivative of the wave action density N and is measured in units of [m²/s]. This term quantifies the rate at which the wave action changes over time, providing insight into the temporal dynamics of wave energy. This equation enables the examination of wave energy transfer and propagation within the Wave Watch III model, contributing to a deeper comprehension of wave climate dynamics and their relevance to wave energy utilization.

The WWIII was applied in this study with a spatial resolution of 0.25° and a temporal resolution of 1 hour. The model domain encompassed the European North East Atlantic region, spanning from 18°S to 80°N in latitude and from -21°W to 10°E in longitude. The simulation period covered a substantial timeframe from January 1, 2003, to December 31, 2012.

To provide the necessary input data for the WWIII model, wind fields derived from the MIROC6 Climate model were utilized. In order to accurately represent the complex nature of wave behavior and wave-to-wave interactions, the model incorporated the discrete interaction approximation (DIA) proposed by Hasselmann et al. in 1985 [25].

In addition, the model employed specific parameterizations known as ST4, as described in the study conducted by Ardhuin et al. in 2010 [26], to account for the influence of wind and wave dissipation source terms within the simulation. These parameterizations were selected to effectively capture the effects of wind and wave dissipation throughout the simulation period.

Recent research [27][28][29][30] highlights the superior performance of the third-generation numerical wind-wave model, WWIII, over reanalysis, satellite, and moored buoys datasets in terms of validating and predicting hindcast and forecast wave climate in both shallow and deep ocean regions. The exceptional accuracy and precision of the WWIII model can be attributed to the explicit definition of non-linear terms and regular updates [31].

$$\frac{\partial N}{\partial t}+\frac{\partial c_x N}{\partial x}+\frac{\partial c_y N}{\partial y}+\frac{\partial c_\sigma N}{\partial \sigma}+\frac{\partial c_\theta N}{\partial \theta}=\frac{S}{\sigma} \quad (2)$$

Wave characteristics are hindcasted at hourly intervals for the years 1992 to 2014. To ensure accuracy, the model run has a warm run, with initiated 15 days before the study period to provide a spin-up period.

D. Domain

The analysis focuses on the North Atlantic European region, spanning from longitude -21W to 10E and latitude 18S to 80N. The model utilizes the General Bathymetric Chart of the Oceans (GEBCO) for bathymetry input and the Global Self-consistent Hierarchical High-Resolution Shorelines (GSHHS) database for shoreline data.

E. Statistical Techniques

1) Normalised Mean Bias (NMB) and Bias

To comprehend the potential performance between the recorded data and reference information, the evaluation is based on the concept of NMB. It is a measure of the average deviation between the modeled (X_{mod}) and the observed (X_{obs}), taking into account the scale of the observed values. This normalization factor ensures that the bias is adjusted proportionally to the magnitude of the observed values, resulting in a standardized measure of deviation. The mathematical expression representing this relationship is as follows:

$$NMB(X)=\frac{\sum(X_{mod}-X_{obs})}{\sum X_{obs}} \quad (3)$$

In addition, to examining the normalized mean bias (NMB), we also evaluate the bias between the recorded data and reference information. Bias provides a measure of the average deviation between the modeled or predicted values and the observed or recorded values, without considering the scale of the observed values. The expression is given below:

$$Bias\ (X)=\sum(X_{mod}-X_{obs}) \quad (4)$$

By incorporating both NMB and bias, a holistic understanding of the potential overestimation or underestimation between the recorded data and reference information, enabling a more thorough assessment of the model's performance.

2) MAE Skill Score (SSMAE)

The skill score by Mean Absolute Error (MAE) approach is employed in this context to evaluate the proficiency of the model, denoted as "X_{ref}" in comparison to the reference data, denoted as "X_{mod}" The calculation is expressed as follows:

$$MAE=\frac{\sum|X_{mod}-X_{ref}|}{n} \quad (5)$$

$$SSMAE = 1 - \frac{MAE}{Mean(X_{ref})} \quad (6)$$

3) IOA

To ensure a thorough check of the assessment, the esteemed Index of Agreement (IOA) is used, meticulously taking into account the presence of bias and variance within the errors [32][33]. The formula for the calculation of this metric is expressed as follows:

$$IOA = 1 - \left(\sum(|X - Y|)^2\right) \div \left(\sum((|X - mean(Y)| + |Y - mean(Y)|^2)\right) \quad (7)$$

The X represents the model estimates and Y represents reference data.

4) KEG

The Kling-Gupta Efficiency (KGE) is a comprehensive statistical metric that was introduced Gupta et al in 2009 [34]. Its purpose is to evaluate the performance of hydrological and hydro-meteorological models by taking into account accuracy, variability, and bias. Unlike the Nash-Sutcliffe Efficiency (NSE) which focuses solely on squared differences, the KGE offers a more comprehensive assessment. This metric finds widespread application in the analysis of climate change impacts and the evaluation of hydrological system fitting performance[35][36]. The KEG is given by,

$$KEG = 1 - \sqrt{[(r-1)^2 + (\beta-1)^2 + (\alpha-1)^2]} \quad (8)$$

r = correlation coefficient
β = bias ratio
α = variability ratio.

5) Wave Power (WP)

The estimation of wave power for an irregular sea state can be described by the following equation, where wave power (WP) is quantified in kilowatts per meter (kW/m) along the wavefront [37].

$$WP = \frac{\rho g^2}{64\pi} T_e (H_{m0})^2 \quad (9)$$

Where ρ is the density of water, g is the acceleration due to gravity , T_e is the wave energy period and H_{m0} is the significant wave height.

III. RESULT AND DISCUSSION

The understanding of ocean wave behavior and its impact on coastal regions is of paramount importance, particularly in the face of climate change and its potential consequences. Accurate and reliable simulations of wave climate serve as critical tools to address these concerns effectively. In this section, the analysis of the spatial patterns for wave climate is presented, with a specific emphasis on significant wave height (hs), employing the state-of-the-art CMIP6 (Coupled Model Intercomparison Project Phase 6) Wave Watch III simulations. Through an examination of the CMIP6 output, insights are derived into the intricate distribution and temporal variability of wave heights across the dynamic domain.

Furthermore, this study undertakes a rigorous evaluation of model performance, encompassing meticulous assessments of bias, normalised mean bias, SSMAE, and a meticulous comparison of observed and simulated wave heights. Additionally, we integrate the application of Index of Agreement (IOA) and Kling-Gupta Efficiency (KEG) as yearly evaluation metrics. This exhaustive analysis aims to foster a robust comprehension of the complex spatial patterns characterizing wave climate, while simultaneously assessing the reliability of the CMIP6 Wave Watch III simulations.

I. Analysis of Normalised Mean Bias, Bias, SSMAE, IOA, and KEG for 2003-2012

To evaluate the accuracy of the simulation, the fifth-generation ECMWF (European Centre for Medium-Range Weather Forecasts) reanalysis dataset, ERA5, was employed as the reference data for the period spanning 2003-2012 [38]. ERA5 combines advanced forecast models and data assimilation systems with a vast amount of observations to produce high-quality reanalysis data [39][40].

Fig 1 illustrates the spatial distribution of bias for the period from January 1, 2003, to December 31, 2012, comparing the significant wave height (Hs) simulated by our model with the reference data (ERA5). The fig highlights regions of underestimation and overestimation in the model's performance in capturing the wave climate. In the North Sea and Norwegian Sea regions, the CMIP6-driven WWIII model consistently underestimates wave heights by an average of 0.3 meters. Similarly, in the Bay of Biscay and the southern part of the English Channel, the model exhibits an underestimation of approximately 0.5 meters.

Conversely, the north-western region of the figure shows an overestimation, which can be attributed to the absence of ice usage in our model compared to ERA5. The inclusion of ice in the ERA5 wave data simulation leads to higher wave heights in this region. The underestimation of wave height observed in our model can be attributed to the absence of swells originating from the North Atlantic, which are not adequately captured by our simulation. This limitation in our model's representation of swell propagation contributes to the overall underestimation of wave heights in the analyzed period.

The presence of temporal coincidence inaccuracies in both the model simulations and the ERA5 wave dataset, combined with the lack of consideration for swells,

contributes to a normalized bias range between -0.25 and 0.25 in Fig 3. This normalized bias indicates a generally favorable agreement between the model outputs and the reference data across the region. However, it is worth noting that the ice forcing from ERA5 introduces discrepancies in certain areas.

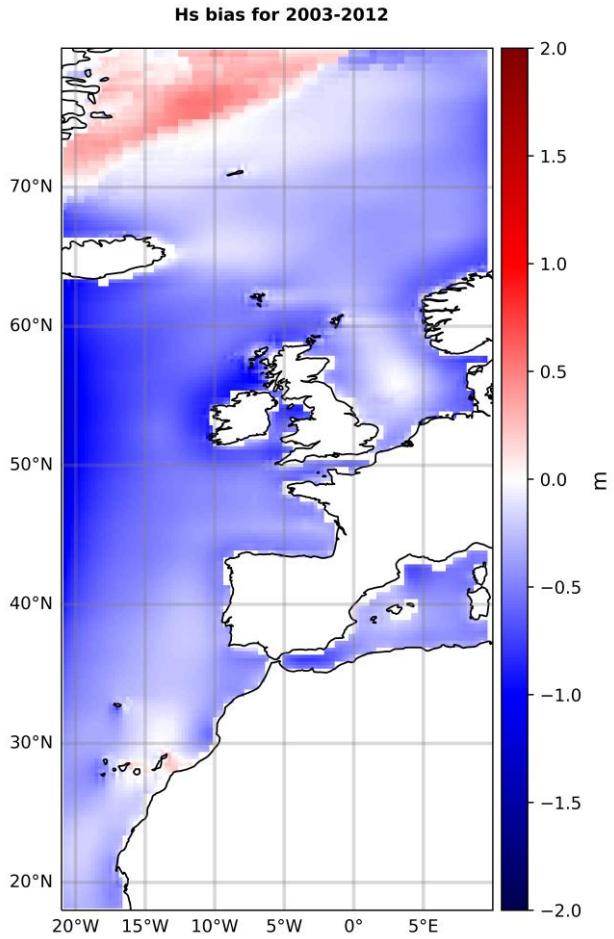

Fig. 1. Spatial distribution of bias (in meters) between significant wave height (hs) simulated by WWIII using MIROC6 winds from CMIP6 and significant wave height (swh) in ERA5 for the period of 2003-2012.

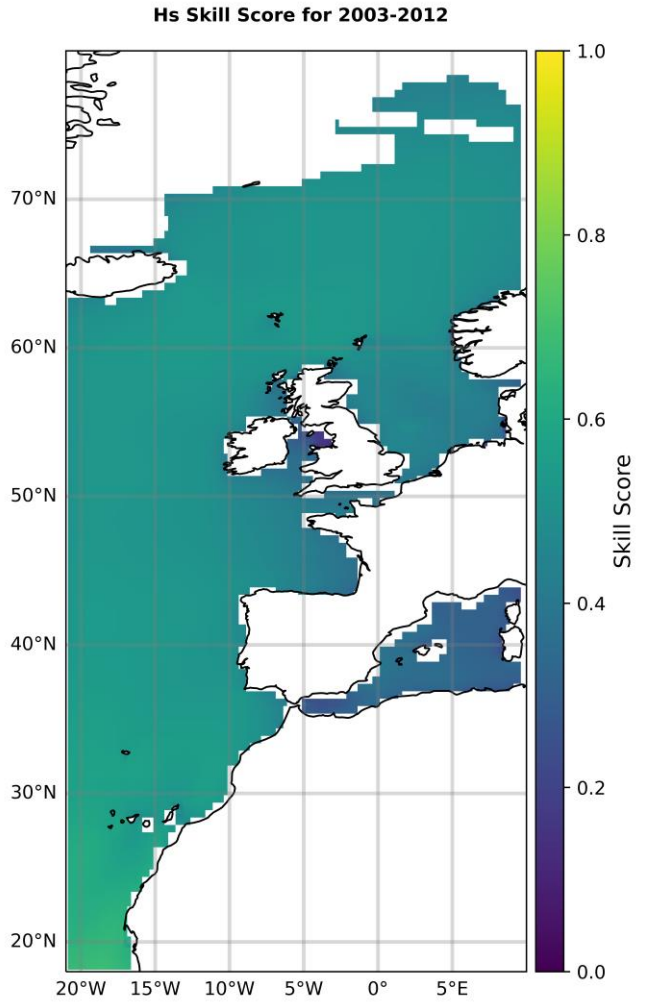

Fig. 2. Illustrates the spatial distribution of the Mean Squared Skill Score (MSSS) between the simulated significant wave height (Hs) obtained from WWIII utilizing MIROC6 winds from CMIP6 and the significant wave height (swh) data in ERA5 from 2003 to 2012.

The evaluation of the mean absolute error skill score demonstrates the proficiency of the CMIP6 WWIII model in simulating significant wave heights, which is crucial for wave energy applications. The obtained scores range from 0.5 to 0.8 across the domain, as illustrated in Fig 2, indicating a moderate to high level of accuracy in reproducing the observed significant wave heights from the ERA5 wave data. Notably, for all years between 2003 and 2012, the model achieves skill scores above the moderate threshold, highlighting its consistent performance and reliability in capturing the wave height characteristics.

Table II provides the yearly significant wave height (Hs) values, along with the corresponding Index of Agreement (IOA) and Kling-Gupta Efficiency (KEG) scores, representing the performance evaluation of the Wave Watch III model utilizing MIROC6 winds from CMIP6. These scores offer a comprehensive assessment of the model's capability to accurately reproduce the observed wave heights throughout the study period.

The IOA scores exhibit a range of 0.80 to 0.89, indicating a significant agreement between the simulated Hs values and the observed wave heights in ERA5. These high IOA scores reflect a robust level of consistency between the model outputs and the reference data, underscoring the model's ability in capturing the wave height variations.

Likewise, the KEG scores span from 0.60 to 0.80, emphasizing the efficiency of the model in replicating the observed wave heights. By incorporating both the variability and magnitude of the wave heights, the KEG scores provide a valuable measure of agreement between the model outputs and the reference data.

The calculation of wave power was conducted on an hourly basis on CMIP6 forced WWIII simulations for the period spanning 1992-2014, shown in Fig 4. The maximum

wave power was observed in 2009 and 2010. The analysis of wave power distribution encompasses both yearly variations and the overall aggregation across the entire study period. The WWIII results based on the MIROC6 model successfully reproduce the spatial variability of wave power, demonstrating distinct regions of high and low power intensity. The maximum predicted power reaches 60 kW/m, indicating the model's capability in capturing the intensity patterns.

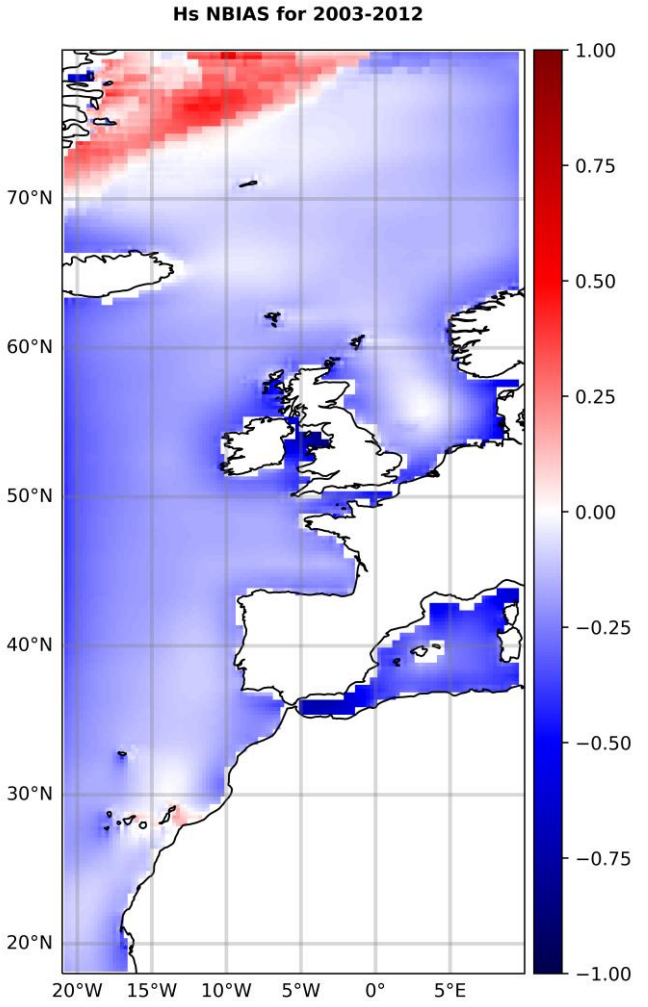

Fig. 3. Spatial distribution of normalized mean bias between significant wave height (hs) simulated by WWIII using MIROC6 winds from CMIP6 and significant wave height (swh) in ERA5 for the period of 2003-2012.

Furthermore, in light of the findings by Reguero [41] suggesting the influence of climate change on wave climate through wind patterns, it is imperative to calibrate and validate the WWIII model, specifically focusing on its ability to simulate climate change dynamics. This calibration and validation process holds significant importance for the wave energy sector, as it enables effective mitigation and adaptation strategies to address the anticipated changes. Therefore, particular attention must be given to refining and improving the WWIII model in the context of climate change analysis, ensuring its applicability and reliability for the wave energy industry.

TABLE II
YEARLY AGGREGATED SPATIAL MEAN VALUES OF SIGNIFICANT WAVE HEIGHT FOR
, IOA, KEG SCORES AND ALL METRICS

YEAR	IOA	KEG	Bias	RMSE	SI	MAE
2003	0.85	0.73	-0.31	0.47	0.21	0.39
2004	0.83	0.64	-0.46	0.55	0.24	0.48
2005	0.88	0.80	-0.23	0.34	0.15	0.27
2006	0.85	0.72	-0.28	0.46	0.20	0.38
2007	0.80	0.61	-0.46	0.59	0.25	0.52
2008	0.80	0.60	-0.51	0.62	0.29	0.55
2009	0.82	0.70	-0.37	0.53	0.22	0.44
2010	0.89	0.80	-0.15	0.31	0.14	0.24
2011	0.81	0.60	-0.54	0.62	0.25	0.56
2012	0.85	0.75	-0.36	0.43	0.19	0.38

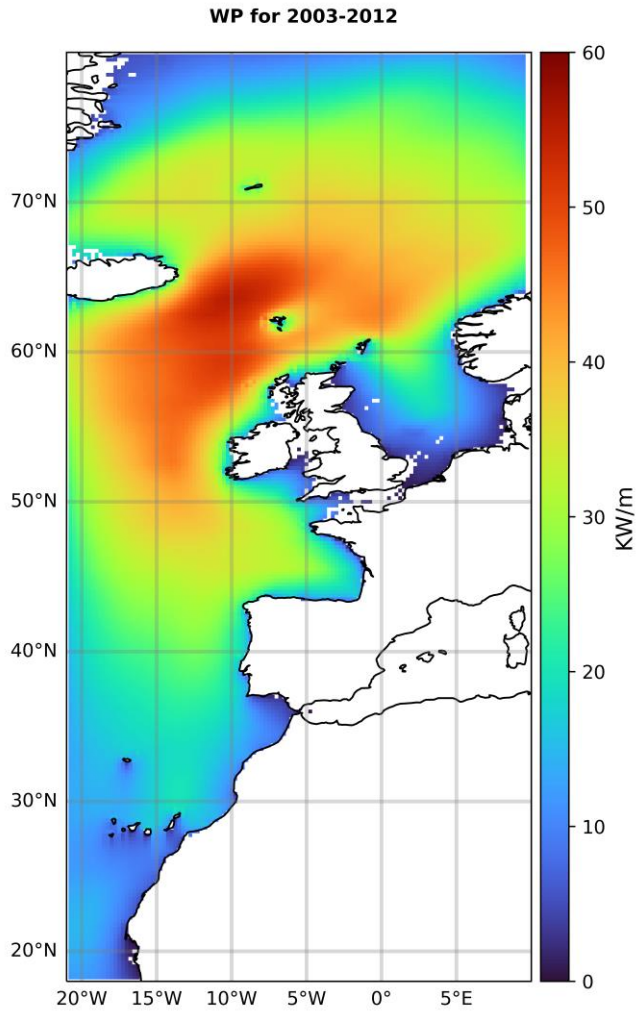

Fig. 4. Illustrates the spatial distribution of the Mean Wave Power(WP) in KW/m for the period of 2003-2012 from MIROC6 forced WWIII.

IV. CONCLUSION

The present study provides valuable insights into the spatial patterns and temporal variations of wave climate, with a specific focus on significant wave height (Hs), utilizing the CMIP6 Wave Watch III simulations. This research in the field of wave energy emphasizes the importance of analyzing wave climate characteristics for assessing wave energy potential. The evaluation of model performance through bias, normalized mean bias, SSMAE, IOA, and KEG metrics highlights the strengths and limitations of the CMIP6-driven WWIII model in reproducing observed wave heights over a 10-year period from 2003 to 2012. The analysis of bias distribution reveals regions of underestimation and overestimation, mainly in the North Sea, Norwegian Sea, Bay of Biscay, and the southern part of the English Channel. These discrepancies can be attributed to the absence of accurate representation of swells and the influence of ice forcing in the reference data (ERA5). Nonetheless, the normalized bias falls within an acceptable range (-0.25 to 0.25), indicating a reasonable agreement between the model outputs and the reference data.

It is important to recognize the limitations of using non-climate model forcing data, such as ERA5, which may not provide a complete understanding of climate change impacts on wave characteristics. Incorporating the CMIP6 MIROC wind data into the model is essential for obtaining a more accurate representation of climate change-induced wave patterns. Fine-tuning the model based on this data will enhance our understanding of the potential effects of climate change on the wave climate in these specific regions.

The observed normalized bias indicates the promising performance of the model in reproducing the wave climate, considering the aforementioned limitations. However, further investigation and fine-tuning, particularly with the inclusion of CMIP6 MIROC6 wind data, are necessary to improve our understanding of the wave climate and its implications for wave energy analysis in the study region. By addressing these factors, we can refine the model's ability to capture the complex dynamics of wave behavior and enhance its accuracy in assessing the impacts of climate change on wave energy resources.

The assessment of mean absolute error skill scores demonstrates the model's ability in reproducing significant wave heights, with scores ranging up to 0.8 across the study domain. The scores indicate a moderate to high level of accuracy in capturing the observed wave heights and validate the model's reliability for wave energy applications. Furthermore, the evaluation of Index of Agreement (IOA) and Kling-Gupta Efficiency (KEG) scores provides additional evidence of the model's capability to accurately replicate wave height variations throughout the study period. The high IOA scores (0.80 to 0.89) and KEG scores (0.60 to 0.80) further underscore the consistency and efficiency of the model in reproducing observed wave heights.

The analysis of wave power distribution reveals distinct regions of high and low power intensity, as captured by the CMIP6-driven WWIII model. The maximum predicted power of 60 kW/m highlights the model's ability to capture the intensity patterns and provides substantial insights for wave energy assessments.

In light of, the findings on the influence of climate change on wave climate through wind patterns, it is crucial to calibrate and validate the WWIII model specifically for climate change analysis. This calibration and validation process will be essential for the wave energy sector and is part of future work, enabling effective mitigation and adaptation strategies to address the anticipated changes. Special attention should be given to refining and improving the model, incorporating climate change dynamics, and ensuring its reliability and applicability for the wave energy industry.

Overall, this study enhances our understanding and highlights the importance of wave climate characteristics, model performance, and the implications of climate change for wave energy applications. These findings contribute to the advancement of wave energy research and provide valuable insights for the effective utilization of wave energy resources in the study region and beyond.

V. ACKNOWLEDGEMENTS

The work has been a part of the EU-SCORES project that has received funding from the European Union's Horizon 2020 research and innovation programme under grant agreement No 101036457.

REFERENCES

[1] Osman, A.I., Chen, L., Yang, M., Msigwa, G., Farghali, M., Fawzy, S., Rooney, D.W. and Yap, P.S., 2022. Cost, environmental impact, and resilience of renewable energy under a changing climate: a review. *Environmental Chemistry Letters*, pp.1-24.

[2] Bethel, B.J. Joint Offshore Wind and Wave Energy Resources in the Caribbean Sea. *J. Marine. Sci. Appl.* **20**, 660–669 (2021). [online].https://doi.org/10.1007/s11804-021-00231-0

[3] Bastos, A., Sippel, S., Frank, D., Mahecha, M.D., Zaehle, S., Zscheischler, J. and Reichstein, M., 2023. A joint framework for studying compound ecoclimatic events. *Nature Reviews Earth & Environment*, pp.1-18.

[4] Bui, H.X., Li, Y.X., Maloney, E.D., Kim, J.E., Lee, S.S. and Yu, J.Y., 2023. Emergence of Madden-Julian oscillation precipitation and wind amplitude changes in a warming climate. *npj Climate and Atmospheric Science*, *6*(1), p.22.

[5] Han, J.H. and Li, J., 2023. Discovery of a New Inter-Basin Climate Pattern: Australia Boundary Current Dipole. *Geophysical Research Letters*, *50*(8), p.e2022GL102715.

[6] Liu, Z. and Alexander, M., 2007. Atmospheric bridge, oceanic tunnel, and global climatic teleconnections. *Reviews of Geophysics*, *45*(2).

[7] Palmer, P.I., Wainwright, C.M., Dong, B., Maidment, R.I., Wheeler, K.G., Gedney, N., Hickman, J.E., Madani, N., Folwell, S.S., Abdo, G. and Allan, R.P., 2023. Drivers and impacts of Eastern African rainfall variability. *Nature Reviews Earth & Environment*, pp.1-17.

[8] Rudeva, I., Boschat, G., Lucas, C., Ashcroft, L., Pepler, A. and Hope, P., 2023. Atmospheric trends explained by changes in frequency of short-term circulation patterns. *Communications Earth & Environment*, *4*(1), p.127.

[9] Dhage, L. and Widlansky, M.J., 2022. Assessment of 21st century changing sea surface temperature, rainfall, and sea surface height patterns in the tropical Pacific Islands using CMIP6 greenhouse warming projections. *Earth's Future*, *10*(4), p.e2021EF002524.

[10] Zelinka, M.D., Myers, T.A., McCoy, D.T., Po-Chedley, S., Caldwell, P.M., Ceppi, P., Klein, S.A. and Taylor, K.E., 2020. Causes of higher climate sensitivity in CMIP6 models. *Geophysical Research Letters*, *47*(1), p.e2019GL085782.

[11] Tokarska, K.B., Stolpe, M.B., Sippel, S., Fischer, E.M., Smith, C.J., Lehner, F. and Knutti, R., 2020. Past warming trend constrains future warming in CMIP6 models. *Science advances*, *6*(12), p.eaaz9549.

[12] Akinsanola, A.A., Ogunjobi, K.O., Abolude, A.T. and Salack, S., 2021. Projected changes in wind speed and wind energy potential over West Africa in CMIP6 models. *Environmental Research Letters*, *16*(4), p.044033.

[13] Goyal, R., Sen Gupta, A., Jucker, M. and England, M.H., 2021. Historical and projected changes in the Southern Hemisphere surface westerlies. *Geophysical Research Letters*, *48*(4), p.e2020GL090849.

[14] Li, J.L., Xu, K.M., Jiang, J.H., Lee, W.L., Wang, L.C., Yu, J.Y., Stephens, G., Fetzer, E. and Wang, Y.H., 2020. An overview of CMIP5 and CMIP6 simulated cloud ice, radiation fields, surface wind stress, sea surface temperatures, and precipitation over tropical and subtropical oceans. *Journal of Geophysical Research: Atmospheres*, *125*(15), p.e2020JD032848.

[15] Charles, E., Idier, D., Delecluse, P., Déqué, M. and Le Cozannet, G., 2012. Climate change impact on waves in the Bay of Biscay, France. *Ocean Dynamics*, *62*, pp.831-848.

[16] Morim, J., Erikson, L.H., Hemer, M., Young, I., Wang, X., Mori, N., Shimura, T., Stopa, J., Trenham, C., Mentaschi, L. and Gulev, S., 2022. A global ensemble of ocean wave climate statistics from contemporary wave reanalysis and hindcasts. Scientific data, 9(1), p.358

[17] Reguero, B.G., Losada, I.J. and Méndez, F.J., 2019. A recent increase in global wave power as a consequence of oceanic warming. Nature communications, 10(1), p.205.

[18] Wang, X.L., Zwiers, F.W. and Swail, V.R., 2004. North Atlantic ocean wave climate change scenarios for the twenty-first century. Journal of climate, 17(12), pp.2368-2383.

[19] Wolf, J. and Woolf, D.K., 2006. Waves and climate change in the north-east Atlantic. *Geophysical Research Letters*, *33*(6).

[20] Lobeto, H., Menendez, M., Losada, I.J. and Hemer, M., 2022. The effect of climate change on wind-wave directional spectra. *Global and Planetary Change*, *213*, p.103820.

[21] Song, T., Liao, H. and Subbarayan, G., 2022. Efficient Local Refinement near Parametric Boundaries Using kd-Tree Data Structure and Algebraic Level Sets. *Algorithms*, *15*(7), p.245.

[22] Mousa, M.H. and Hussein, M.K., 2022. Toward high-performance computation of surface approximation using a GPU. *Computers and Electrical Engineering*, *99*, p.107761.

[23] Tatebe, H., Ogura, T., Nitta, T., Komuro, Y., Ogochi, K., Takemura, T., Sudo, K., Sekiguchi, M., Abe, M., Saito, F. and Chikira, M., 2019. Description and basic evaluation of simulated mean state, internal variability, and climate sensitivity in MIROC6. *Geoscientific Model Development*, *12*(7), pp.2727-2765.

[24] Kataoka, T., Tatebe, H., Koyama, H., Mochizuki, T., Ogochi, K., Naoe, H., Imada, Y., Shiogama, H., Kimoto, M. and Watanabe, M., 2020. Seasonal to decadal predictions with MIROC6: Description and basic evaluation. *Journal of Advances in Modeling Earth Systems*, *12*(12), p.e2019MS002035.

[25] Hasselmann, S., Hasselmann, K., Allender, J.H. and Barnett, T.P., 1985. Computations and parameterizations of the nonlinear energy transfer in a gravity-wave specturm. Part II: Parameterizations of the nonlinear energy transfer for application in wave models. *Journal of Physical Oceanography*, *15*(11), pp.1378-1391.

[26] Ardhuin, F., Rogers, E., Babanin, A., Filipot, J.-F., Magne, R., Roland, A., van der Westhuysen, A., Queffeulou, P., Lefevre, J.-M., Aouf, L., and Collard, F.: Semi-empirical dissipation source functions for wind-wave models: part I, definition, calibration and validation, J. Phys. Oceanogr., 40, 1917–1941, [online] https://doi.org/10.1175/2010JPO4324.1, 2010.

[27] Beyramzadeh, M., Siadatmousavi, S.M. and Derkani, M.H., 2021. Calibration and skill assessment of two input and dissipation parameterizations in WAVEWATCH-III model forced with ERA5 winds with application to Persian Gulf and Gulf of Oman. *Ocean Engineering*, *219*, p.108445.

[28] Bi, F., Song, J., Wu, K. and Xu, Y., 2015. Evaluation of the simulation capability of the Wavewatch III model for Pacific Ocean wave. *Acta Oceanologica Sinica*, *34*, pp.43-57.

[29] Kazeminezhad, M.H. and Siadatmousavi, S.M., 2017. Performance evaluation of WAVEWATCH III model in the Persian Gulf using different wind resources. *Ocean Dynamics*, *67*, pp.839-855.

[30] Mentaschi, L., Besio, G., Cassola, F. and Mazzino, A., 2015. Performance evaluation of Wavewatch III in the Mediterranean Sea. *Ocean Modelling*, *90*, pp.82-94.

[31] Cavaleri, L., Alves, J.H., Ardhuin, F., Babanin, A., Banner, M., Belibassakis, K., Benoit, M., Donelan, M., Groeneweg, J., Herbers, T.H.C. and Hwang, P.A.E.M., 2007. Wave modelling–the state of the art. *Progress in oceanography*, *75*(4), pp.603-674.

[32] Jeong, G.R., Baker, B., Campbell, P.C., Saylor, R., Pan, L., Bhattacharjee, P.S., Smith, S.J., Tong, D. and Tang, Y., 2023. Updating and Evaluating Anthropogenic Emissions for NOAA's Global Ensemble Forecast Systems for Aerosols (GEFS-Aerosols): Application of an SO2 Bias-Scaling Method. *Atmosphere*, *14*(2), p.234.

[33] Khatti, J. and Grover, K.S., 2023. Prediction of UCS of fine-grained soil based on machine learning part 1: multivariable regression analysis, gaussian process regression, and gene expression programming. *Multiscale and Multidisciplinary Modeling, Experiments and Design*, pp.1-24.

[34] Gupta, H.V., Kling, H., Yilmaz, K.K. and Martinez, G.F., 2009. Decomposition of the mean squared error and NSE performance criteria: Implications for improving hydrological modelling. *Journal of hydrology*, *377*(1-2), pp.80-91.

[35] Becker, R., Koppa, A., Schulz, S., Usman, M., aus der Beek, T. and Schüth, C., 2019. Spatially distributed model calibration of a highly managed hydrological system using remote sensing-derived ET data. *Journal of Hydrology*, *577*, p.123944.

[36] Daba, M.H. and You, S., 2020. Assessment of climate change impacts on river flow regimes in the upstream of Awash Basin, Ethiopia: based on IPCC fifth assessment report (AR5) climate change scenarios. *Hydrology*, *7*(4), p.98.

[37] Reguero, B.G., Losada, I.J. and Méndez, F.J., 2019. A recent increase in global wave power as a consequence of oceanic warming. Nature communications, 10(1), p.205.

[38] Hersbach, H., Bell, B., Berrisford, P., Hirahara, S., Horányi, A., Muñoz-Sabater, J., Nicolas, J., Peubey, C., Radu, R., Schepers, D. and Simmons, A., 2020. The ERA5 global reanalysis. Quarterly Journal of the Royal Meteorological Society, 146(730), pp.1999-2049.

[39] Bidlot, J.R., Abdalla, S. and Hersbach, H., 2017, April. ERA5 wave data. In *EGU General Assembly Conference Abstracts* (p. 8707).

[40] Bruno, M.F., Molfetta, M.G., Totaro, V. and Mossa, M., 2020. Performance assessment of ERA5 wave data in a swell

dominated region. *Journal of Marine Science and Engineering*, *8*(3), p.214.

[41] Reguero, B.G., Losada, I.J. and Méndez, F.J., 2019. A recent increase in global wave power as a consequence of oceanic warming. Nature communications, 10(1), p.205.